SRTTU

JCARME
ISSN: 2228-7922

Journal of Computational and Applied Research
in Mechanical Engineering
Vol. 5, No. 1, pp. 61- 69, Autumn-Winter 2015-16
jcarme.srttu.edu

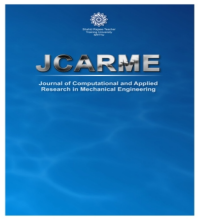

Internal combustion engines in cylinder flow simulation improvement using nonlinear k-ε turbulence models

A. Mirmohammadi[a,] * and F. Ommi[b]

[a]*Department of Mechanical Engineering, Shahid Rajaee Teacher Training University, Lavizan, Tehran*
[b]*Department of Mechanical Engineering, Tarbiat Modares University, Tehran*

Article info:
Received: 19/01/2015
Accepted: 26/04/2015
Online: 11/09/2015

Keywords:
Engine,
Flow,
Simulation,
Nonlinear k-ε ,
Turbulence model.

Abstract
The purpose of this paper is to studying nonlinear k-ε turbulence models and its advantages in internal combustion engines, since the standard k-ε model is incapable of representing the anisotropy of turbulence intensities and fails to express the Reynolds stresses adequately in rotating flows. Therefore, this model is not only incapable of expressing the anisotropy of turbulence in an engine cylinder, but also is unable to provide good performance when computing the swirling and tumbling flows is important in engine cylinders. Thus, in this paper, the results of nonlinear k-ε model are compared with those of the linear one. Results of diesel engine simulation with linear and nonlinear k-ε models in comparison show that turbulence intensity in the nonlinear model simulation is higher than that of the linear model; also, nonlinear k-ε models predict the second peak value because of the bowl shape in expansion stroke for turbulence intensity. Gas injection results show that nonlinear turbulence models predict spray penetration accurately because of correctly turbulence intensities predicting. Also, the results demonstrate that, for high pressure gas injection, turbulence intensity is high and predicted accurately using nonlinear models. Then, its spray penetration length is predicted accurately in comparison to experimental data's. Although CPU time spending in the nonlinear model is more than that of the linear one, the non-linear stress model is found to increase computation time by 19%.

1. Introduction

Turbulence modeling is still one of the most, if not the most, critical issues when approaching engineering flow CFD simulations of practical interest. Turbulence modeling is even more difficult when considering internal combustion engines (ICE), which may be related to the combination of high Reynolds numbers and complex geometries, where streamline curvature and separation have significant effects. The engine flows are intrinsically very complex in nature, because they have more than one dynamically varying strains.

Therefore, one of the feasible approaches for the evaluation of engineering flows is to solve the Reynolds-averaged Navier Stokes (RANS) equations in conjunction with a turbulence

*Corresponding author
Email address: a.mirmohammadi@srttu.edu

model. While neglecting one-equation turbulence models because of their lack of generality, on the one side, and the second moment closure models because of their computational expensiveness, on the other side, nowadays, the use of two-equation linear and nonlinear eddy viscosity models (hereafter referred to as simply EVM) represents an unavoidable compromise between computational cost and accuracy. Despite the fact that linear EVMs are widely used, they can provide only general information on turbulence behavior. Linear EVMs have been and are still widely criticized due to the lack of physical background of both constitutive relation, based on the Boussinesq hypothesis, and the near-equilibrium hypothesis. Nonlinear EVMs, on the other hand, are affected by stronger numerical instability; however, they represent good compromise between the physical fundaments of the second moment closures (i.e. RSM) and the low computational complexity of linear EVMs [1]. Nevertheless, although several two-equation nonlinear EVM turbulence models can be found in the literature, in quadratic and cubic expansion (even quadratic), differing for underlying hypotheses, formulation, complexity, and degree of accuracy, none of them can provide the necessary predictive capability and generality of use and still require a certain degree of case by case tuning.

The recognition that linear k-ε model cannot provide satisfactory predictions in complex flows has pushed researchers towards the development of nonlinear EV turbulence models. Meanwhile, LES is becoming feasible for complex engineering problems; a fashionable and theoretically more accurate simulation of turbulence within RANS approach is represented using non-linear k-ε models, as very interesting compromise between the linear k-ε model and the Reynolds-stress model. Nonlinear k-ε models are characterized by a nonlinear stress-strain constitutive relation where the Reynolds-stress components are obtained as the non-linear expansion of strain rate and vorticity components. The nonlinear k-ε models are developed in order to overcome some of the limitations of the linear constitutive relation related to the Boussinesq hypothesis. The general constitutive correlation was first provided by Pope by means of the application of the generalized Caley-Hamilton formulas to the shear and rotation tensors [2].

The impact of a nonlinear turbulent stress relationship on the simulations of flow and combustion in an HSDI diesel engine was studied in [3]. The results were confirmed by the results of motored flow simulations, in which the mean flow structures and the spatial distribution of turbulent kinetic energy were not observed to vary significantly until expansion was underway. Globally, the magnitude of the turbulent kinetic energy is typically less when the nonlinear stress model is employed and the turbulent time scales are larger. Also, their results showed that, with fuel injection, the velocities along the jet axis were strongly affected by the turbulence model, indicating the differences in the entrainment and mixing rates that were consistent with the predicted differences in the early heat release characteristics. Subsequent deflection of the jet at the bowl wall led to differences in the mean flow structures in the bowl and resulted in changes to both the heat release rate and the spatial distribution of soot. Structural differences in the mean flow were also observed in the squish volume during the expansion. Moreover, they demonstrated that the use of the nonlinear stress model could increase computation times by 15-38%.

Both second-moment closure and third-order nonlinear eddy viscosity turbulence models were studied in [4]. The results of the RNG k-ε model demonstrated that the computational values of the eddy diffusivity were smaller than those of the nonlinear models, especially during the later period of an expansion stroke. Also, concerning computational time, the three-order nonlinear model needed up to 1.2 times of the standard k-ε model.

In this research, a nonlinear eddy viscosity model, which is expected to show better performance than the linear eddy viscosity model (the standard k-ε model) in swirling and tumbling flows in engine cylinders, is

incorporated into the engine CFD code KIVA-3V [5-7].

2. Governing equations

The governing equations in flow simulation are summarized as follows:

$$\frac{\partial \rho_m}{\partial t} + \nabla \cdot (\rho_m U) = \nabla \cdot \left[\rho D_t \nabla \left(\frac{\rho_m}{\rho} \right) \right] + \dot{\rho}_m^c \quad (1)$$

$$\frac{\partial (\rho U)}{\partial t} + \nabla \cdot (\rho U U) = -\frac{1}{\alpha^2} \nabla P - A_0 \nabla (2/3 \rho k) + \nabla \cdot \sigma + \rho g \quad (2)$$

$$\sigma = \mu_{eff} [\nabla U + (\nabla U)^T] - \frac{2}{3} \mu_{eff} \nabla \cdot U \bar{I} \quad (3)$$

$$\mu_{eff} = \mu + \mu_t \quad (4)$$

$$\frac{\partial (\rho I_{\text{int}})}{\partial t} + \nabla \cdot (\rho U I_{\text{int}}) = -P \nabla \cdot U + (1 - A_0) \sigma \nabla U - \nabla \cdot J + A_0 \rho \varepsilon + \dot{Q}^c + \dot{Q}^g \quad (5)$$

$$J = -K \nabla T - \rho D_t \sum_m h_m \nabla \left(\frac{\rho_m}{\rho} \right) \quad (6)$$

2. 1. Turbulence models

The turbulence models in the present work are linear k-ε and nonlinear k-ε models. These models are easily applicable to real flows with complex geometry. Below, we explain the nonlinear k-ε and stress transport models.

2.2. Overview of k-ε turbulence model

The applied KIVA code has a generalized standard turbulence model. The standard k-ε turbulence model is given as follows:
Turbulence kinetic energy:

$$\frac{\partial}{\partial t} \left(\bar{\rho} \tilde{k} \right) + div \left(\bar{\rho} \tilde{u} \tilde{k} \right) = div \left[\frac{\mu_T}{\sigma_k} grad \tilde{k} \right] + \bar{\rho} \bar{p}_k - \bar{\rho} \tilde{\varepsilon} \quad (7)$$

Dissipation rate of kinetic energy:

$$\frac{\partial}{\partial t} \left(\bar{\rho} \tilde{\varepsilon} \right) + div \left(\bar{\rho} \tilde{u} \tilde{\varepsilon} \right) = div \left[\frac{\mu_T}{\sigma_\varepsilon} grad \tilde{\varepsilon} \right] + C_{1\varepsilon} \frac{\tilde{\varepsilon}}{\tilde{k}} \bar{p}_k - C_{2\varepsilon} \bar{\rho} \frac{\tilde{\varepsilon}^2}{\tilde{k}} + \bar{\rho} C_{3\varepsilon} \tilde{\varepsilon} \nabla . u \quad (8)$$

in which $\varepsilon = \tilde{\varepsilon} + D$;
where k is the turbulent kinetic energy; ε is the turbulent kinetic energy dissipation rate, the conventional turbulence model constants are $C_{1\varepsilon}$ =1.45, $C_{2\varepsilon}$ = 1.92, $C_{3\varepsilon}$ = 1, σ_k = 1, σ_ε = 0.7, and $\mu_T = C_\mu \frac{k^2}{\varepsilon}$, C = 0.09, and D are the diffusion terms.

$$\bar{p}_k = -\bar{\rho} \overline{u_i'' u_j''} \frac{\partial \tilde{u}_i}{\partial x_j} \quad (9)$$

Reynolds stress in the standard k-ε turbulence model is given below:

$$-\bar{\rho} \overline{u_i'' u_j''} = -\frac{2}{3} \left(\bar{\rho} \tilde{k} + \mu_T \frac{\partial \tilde{u}_k}{\partial x_k} \right) \delta_{ij} + \mu_T \left(\frac{\partial \tilde{u}_i}{\partial x_j} + \frac{\partial \tilde{u} j}{\partial x_i} \right) \quad (10)$$

In this work, the standard k-ε model is improved using nonlinear relation for stress tensor; this modified k-ε model is called nonlinear k-ε turbulence model. The modification to the equation is given as follows: Stress tensor in nonlinear k-ε turbulence model is given in Eq. (11) [8, 9].

$$\begin{aligned} \overline{u_i'' u_j''} = & -2 v_T S_{ij} + \frac{2}{3} \tilde{k} \delta_{ij} + C_1 v_T \frac{\tilde{k}}{\tilde{\varepsilon}} (S_{ik} S_{kj} - \frac{1}{3} S_{kl} S_{kl} \delta_{ij}) + C_2 v_T \frac{\tilde{k}}{\tilde{\varepsilon}} (\Omega_{ik} S_{kj} + \Omega_{jk} S_{ki}) + \\ & C_3 v_T \frac{\tilde{k}}{\tilde{\varepsilon}} (\Omega_{ik} \Omega_{jk} - \frac{1}{3} \Omega_{lk} \Omega_{lk} \delta_{ij}) + \\ & C_4 v_T \frac{\tilde{k}^2}{\tilde{\varepsilon}^2} (S_{ki} \Omega_{lj} + S_{kj} \Omega_{li}) S_{kl} + \\ & C_5 v_T \frac{\tilde{k}^2}{\tilde{\varepsilon}^2} (\Omega_{il} \Omega_{lm} S_{mj} + S_{il} \Omega_{lm} \Omega_{mj} - \frac{2}{3} S_{lm} \Omega_{mn} \Omega_{nl} \delta_{ij}) + C_6 v_T \frac{\tilde{k}^2}{\tilde{\varepsilon}^2} S_{ij} S_{kl} S_{kl} \\ & + C_7 v_T \frac{\tilde{k}^2}{\tilde{\varepsilon}^2} \Omega_{kl} \Omega_{kl} \end{aligned} \quad (11)$$

where:

$$\Omega_{ij} = \frac{1}{2} \left(\frac{\partial \tilde{u}_i}{\partial x_j} - \frac{\partial \tilde{u}_j}{\partial x_i} \right)$$

$$S_{ij} = \frac{1}{2} \left(\frac{\partial \tilde{u}_i}{\partial x_j} + \frac{\partial \tilde{u}_j}{\partial x_i} \right), \quad v_T = C_\mu f_\mu \frac{\tilde{k}^2}{\tilde{\varepsilon}}$$

In these equations, Reynolds stress in nonlinear k-ε turbulence model has two parts: Part 1 includes two order stress tensor and Part 2 includes three order stress tensors so that, if three components of vorticity rate (Ω) and strain rate (S) are the product, it is three order k-ε model and, if this product is twice, it is two order nonlinear k-ε turbulence model.

In these equations, C_μ is optimum eddy viscosity factor and its relation with strain and vorticity is as follows:

$$C_\mu = \frac{0.3}{1+0.35(\max(S,\Omega))^{1.5}} \times \left(1-\exp\left[\frac{-0.36}{\exp(-0.75\max(S,\Omega))}\right]\right) \quad (12)$$

where:

$$S = \frac{k}{\varepsilon}\sqrt{1/2\, S_{ij}S_{ij}} \quad , \quad \Omega = \frac{k}{\varepsilon}\sqrt{1/2\, \Omega_{ij}\Omega_{ij}}$$

At high Reynolds numbers, the constants are as shown below [4]:

$$C_1 = -0.2, \quad C_2 = 0.4, \quad C_3 = 2-\exp(-(S-\Omega)^2),$$
$$C_4 = -32C_\mu^2, C_5 = 0, \quad C_6 = -16C_\mu^2, \quad C_7 = 16C_\mu^2,$$
$$f_\mu = 1.0$$

The second-order terms are related to the anisotropy of the Reynolds stress; but, the second-order nonlinear k-ε model cannot reproduce the rotation and curvature effects. Since the third-order terms including the vorticity effects are closely connected with the first-order eddy viscosity term, there is strong possibility that the third-order nonlinear k-ε model predicts a variety of turbulent flows correctly.

3. Boundary conditions and nonlinear model

In near wall, flow influenced with wall and its speed is reduced. This act reduces Reynolds number. A simple method for studying wall effect is done by assuming wall flow as laminar and one dimensional. Also it is assuming that near wall strain be constant and equal to wall strain.

Thus in k-ε model for given boundary conditions, boundary layers divided to two layer: viscous and inners layer. Then Von Karman laws are used for dimensionless length and velocity variables. Also it is assumed varying of eddies length has linear relation with distance from wall. Kinetic energy in wall defines as below:

$$\tilde{k} = \sqrt{C_\mu}\,\tau_w / \overline{\rho} \quad (13)$$

In this equation, C_μ is constant for standard k-ε; but, in nonlinear k-ε model, it is defined as variable and completely different. Thus, flow conditions are prospected accurately at the boundary using nonlinear k-ε model.

4. Results of modified KIVA-3V code

For code modification, the linear Reynolds stress model formula and its constants are replaced by nonlinear model (Eq. (11)) in turbulence subroutine in KIVA-3V Code. In the modified code, the Reynolds stress is computed using nonlinear eddy viscosity and it needs more CPU time because of computing high order algebraic terms in nonlinear k-ε model. But, compared with other methods such as RSM in which more equations should be solved, it is not considered great time. In this work, the result of main and modified codes for simulation in the cylinder flow of diesel engine and gas direct injection is analyzed.

4. 1. Performance of new turbulence model in diesel chamber

The OM-355 diesel engine is used for the analysis and the data are shown in Table 1. Simulation is done for 1400rpm engine speed. In the cylinder, mesh generation in Fig. 1 is done separately in ICEM-CFD software. The simulation is performed for closed-valves cycle: from closing inlet valve at 240°CA after top dead center to opening exhaust valve at 472°CA. Initial swirl ratio is assumed zero,

initial cell turbulence kinetic energy density is 0.6, and initial turbulence length scale is 0.82.

Table 1. Characteristics of OM-355 diesel engine.

Diameter	128mm
Engine capacity	11.58 Lit
Compression ratio	16.1
Stroke	150mm

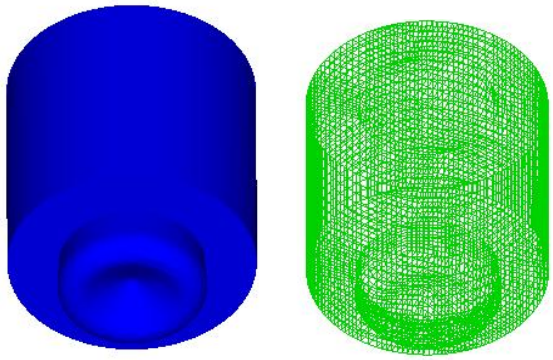

Fig. 1. Chamber mesh generated in ICEM-CFD.

4. 1. 1. Initial and boundary conditions

OM-355 diesel engine's initial and boundary conditions at 1400 rpm engine speed are given in Table 2.

Table 2. OM-355 engine's initial and boundary condition values at 1400 rpm.

In cylinder initial temperature	400K	In cylinder initial pressure	1.55bar
Cylinder walls constant temperature	475K	Cylinder Head walls constant temperature	500K
Piston Crown walls constant temperature	525K		

4. 1. 2. Grid independency for simulating diesel chamber

The grid independency results are shown in Tables 3 and 4. For all the cases, constant values are taken for injection speed and total mass of injection are 1400rpm engine speed and spray tip penetration length after 1 msec in Table 2 along with maximum incylinder pressure in Table 3 is considered the criterion values. The results show that the answer for 40000 grid number is slightly different from the 50000 one and the difference between 40000 and 30000 is great. Then, 40000 grid number is selected for solution.

Table 3. Results of independency from grid numbers.

Grid Numbers	Injection Velocity (cm/sec)	Total Injection Mass (gr)	Spray Penetration after 1msec (mm)
30000	18500	0.112	29.3
40000	18500	0.112	33.6
50000	18500	0.112	33.9

Table 4. Results of independency from grid numbers.

Grid Numbers	Injection Velocity (cm/sec)	Total Injection Mass (gr)	Maximum in cylinder pressure
30000	18500	0.112	65.1
40000	18500	0.112	60.9
50000	18500	0.112	60.3

4. 1. 3. Incylinder flow simulation

Figures 2 and 3 show the flow vectors' distribution inside the cylinder in compression stroke. It is seen that flow circulation is predicted using both linear and nonlinear k-ε turbulence models. For compression stroke, the differences observed in the predictions of mean flow development are small and do not emerge until expansion.

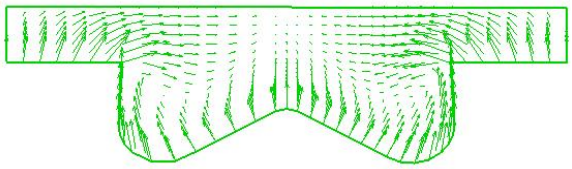

Fig. 2. Incylinder flow speed vectors in compression stroke predicted by the main code.

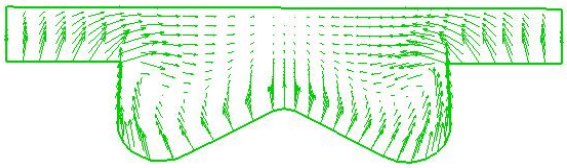

Fig. 3. Incylinder flow speed vectors in compression stroke predicted using modified code.

Figures 4 and 5 demonstrate the distributions of flow speed vectors in expansion stroke, resulted from the main and modified codes, respectively.

It can be observed in these figures that both turbulence models truly predict flow directions inside the cylinder. Accurate analysis shows that modified code predicts flow direction better than the main code in near-wall flows in Fig. 5. Larger differences are found in the spatial distribution and magnitude of turbulent kinetic energy. The nonlinear model generally predicts lower energy levels and larger turbulent time scales.

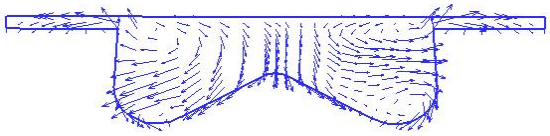

Fig. 4. Incylinder flow speed vectors in expansion stroke predicted using the modified code.

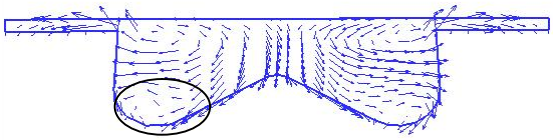

Fig. 5. Incylinder flow speed vectors in expansion stroke predicted using the modified code.

Figures 6 and 7 show incylinder turbulent kinetic energy for OM-355 engine that is simulated respectively by main and modified codes.

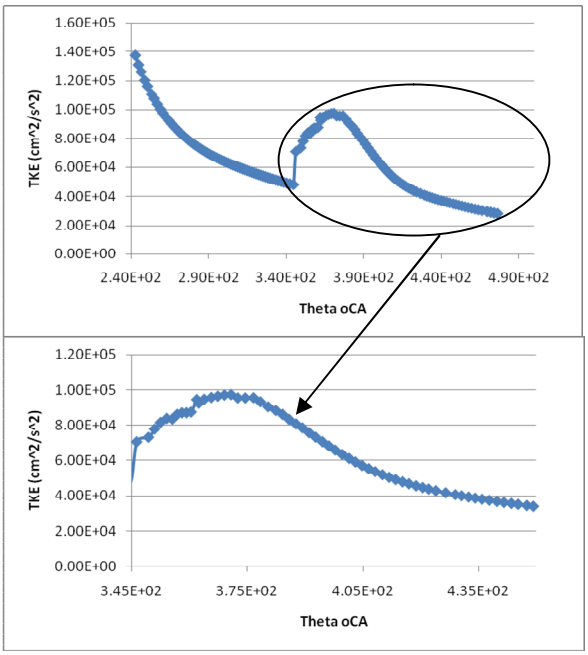

Fig. 6. Incylinder flow kinetic energy predicted using the main code.

It can be found that both linear and nonlinear k-ε models truly predict the increase of turbulence intensity because of injection phenomena; but, another maximum point is predicted by nonlinear k-ε model because of its bowl shape. Also, accurate analysis of Figs. 6 and 7 show that nonlinear k-ε model predicts the amount of turbulent energy more than the linear model.

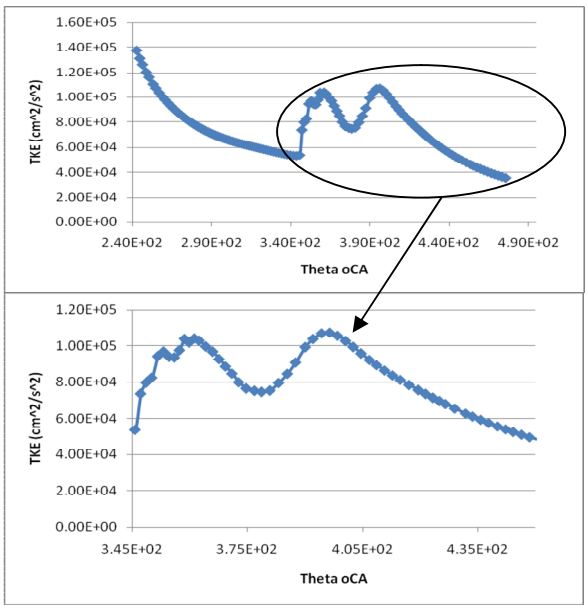

Fig. 7. Incylinder flow kinetic energy predicted using the modified code.

4. 2. Performance of new turbulence model in gas direct injection

Constant volume combustion chamber that is shown in Fig. 8 is simulated using the main and modified codes.

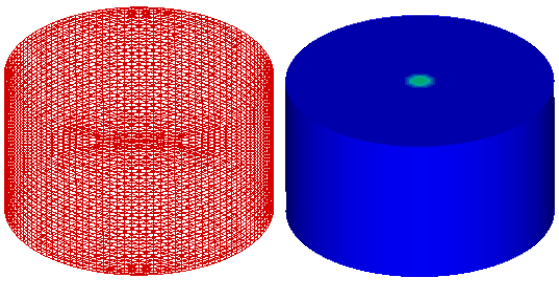

Fig. 8. Constant volume chamber meshing.

The chamber specification is presented in Table 5. Also, the initial and boundary conditions are shown in Table 6.

Table 5. Simulated constant volume combustion chamber and nozzle specifications.

Combustion chamber specifications	Quantity
Cylinder bore	123 mm
Cylinder high	70 mm
Nozzle hole number	1
Hole diameter	0.5 mm
Injection angle	Normal to down

Table 6. Combustion chamber and nozzle's initial and boundary conditions [10].

specifications	Quantity
Combustion chamber initial temperature	298 k
Combustion chamber initial pressure	15 bar
Injection initial temperature	310 k
Injection pressure	22.5 bar

4. 2. 1. Grid independency for gas injection in constant volume chamber

The grid independency results are shown in Table 7. For all cases, constant values are taken for speed and mass flow rate and time for 70mm spray tip penetration is considered a criterion value. The results show that the answer for 100000 grid number is slightly different from the 180000 one and the difference between 100000 and 36000 is great. Then, the 100000 grid number is selected for the solution.

Table 7. Studying independency of results from grid numbers.

Grid Numbers	Injection Velocity (m/sec)	Injection Mass Flow Rate(gr/sec)	Time For 70mm Spray Penetration(msec)
180340	701.26	53.517	0.816122
100280	701.26	53.517	0.82159
48220	701.26	53.517	0.828859
36200	701.26	53.517	0.853241

4. 2. 2. Gas injection in constant volume simulation

Methane gas spray penetration was simulated using linear (top) and three degree nonlinear turbulence model (bottom) that was shown in Fig. 9. The gas penetration was defined as distance from the injection point to the point that fuel mass fraction is 0.003. It is seen that nonlinear model with predicting adequate turbulence flow has better mixing and low penetration length in comparison to linear one.

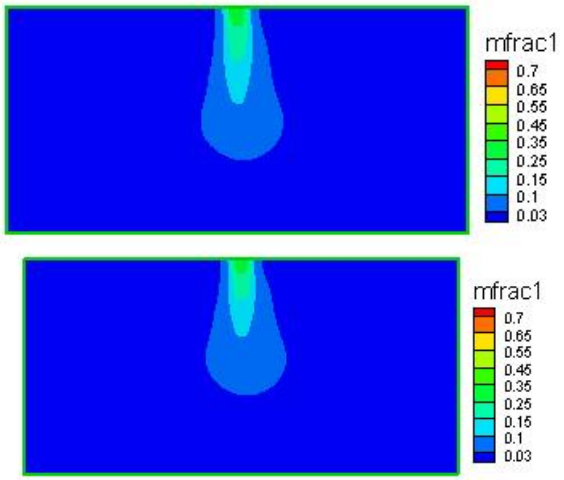

Fig. 9. Gas spray penetration length after 3 msec using linear (top) and nonlinear (bottom) turbulence models.

Gas spray penetration that is simulated using linear k-ε turbulence model in comparison to the experimental results of reference [6] is presented in Fig. 10. Figures 11 and 12 show the results of the simulated penetration for two- and three-degree nonlinear turbulence models in comparison to the experimental results.

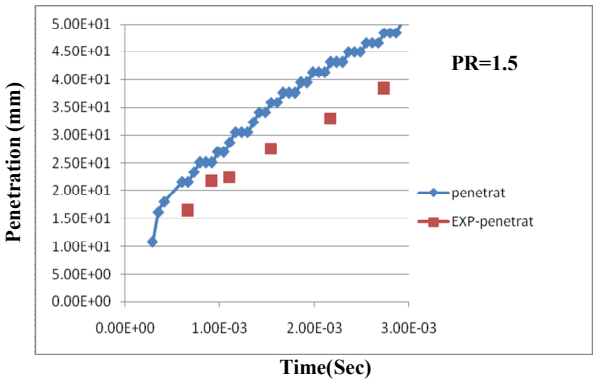

Fig. 10. Comparison of spray penetration with linear turbulence model simulation to the experimental results.

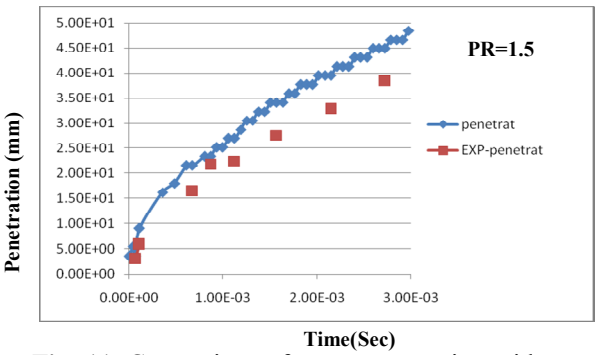

Fig. 11. Comparison of spray penetration with two-degree nonlinear turbulence model simulation to the experimental results.

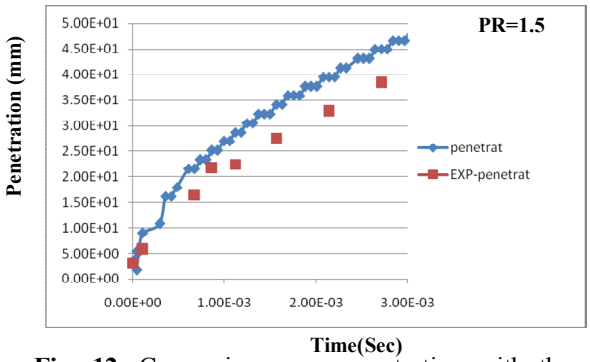

Fig. 12. Comparing spray penetration with three-degree nonlinear turbulence model simulation to the experimental results.

Table 8. Data of simulation results in Figs. 10, 11 and 12.

Injection pressure ratio	Duration time after injection	Experimental penetration	Penetration with linear turbulence model simulation	Percent error	Penetration with two degree nonlinear turbulence model simulation	Percent error	Penetration with two degree nonlinear turbulence model simulation	Percent error
1.5	2.73	38.5	48.1299	25	44.8718	16.55	44.8718	16.55
1.5	2.15	32.9	42.3602	28.75	39.4872	20	39.4872	20
1.5	1.57	27.5	35.8974	30.538	34.1026	24.01	34.1026	24.01
1.5	0.671	16.2	21.7226	34.1	21.5384	32.95	21.5384	32.95
1.5	2.21	47.8	57.436	20.16	54.9786	15	55.3129	15.7
1.5	1.65	40	48.7184	21.2	46.6667	16.6	46.6667	16.6
1.5	1.05	31.4	38.5988	22.9	37.6923	20.04	37.6923	20.04
1.5	0.492	20.1	25.1281	25	25.1281	25	24.7442	23
1.5	1.33	45.7	48.3229	5.7	45.8718	0.3	45.9105	0.46
1.5	1.09	40.7	43.077	5.8	41.2821	1.4	41.2821	1.4
1.5	0.875	34	38.1173	12	35.8974	5.58	36.1543	6.3

The results show that simulated penetration using nonlinear turbulence models is near the experimental value, because it has better mixing and lower penetration than the linear one.

The data of Figs. 10, 11, and 12 are presented numerically in Table 8 to make a better comparison.

It is seen from this table that, for higher injection pressure, turbulence intensity is high and nonlinear models predict accurately; also, they can better predict penetration length.

5. Conclusions

Nonlinear and standard k-ε turbulence models were used for internal combustion diesel engines in cylinder flow simulation and the results showed that:

1- Nonlinear k-ε model needed more CPU time because of computing high order algebraic terms in the model. The use of the non-linear stress model was found to increase computation times by 19%.

2- Both linear and nonlinear k-ε turbulence models truly predicted flow direction inside the cylinder.
3- Nonlinear k-ε predicted turbulence flows better than the main code in near-wall mode.
4- It was seen that both linear and nonlinear k-ε models truly predicted the increase of turbulence intensity because of injection phenomena.
5- Results showed that nonlinear k-ε models predicted second-peak value because of bowl shape in the expansion stroke for turbulence intensity.
6- Results also demonstrated that nonlinear k-ε model predicted the energy amount of peak turbulent kinetics more than linear model.
7- Gas injection results showed that nonlinear turbulence models predicted spray penetration accurately and better predicted turbulence intensities.
8- For higher injection pressure, turbulence intensity was high and nonlinear models predicted accurately. Also, they could better predict penetration length.

References

[1] G. M. Bianchi et al, "Turbulence Modeling in CFD Simulation of ICE Intake Flows: The Discharge Coefficient Prediction", *SAE*, 2002-01-1118.

[2] D. D. Apsley and M. A. Leschziner, "A new Low-Reynolds-Number Nonlinear Two-Equation Turbulence Model for Complex Flows", *International Journal of Heat and Fluid Flow*, Vol. 19 No. 5, pp. 209-222, (1998).

[3] R. D. Reitz et al, "The Impact of a Non-Linear Turbulent Stress Relationship on Simulations of Flow and Combustion in an HSDI Diesel Engine", *SAE*, 2008-01-1363.

[4] M. Okamoto et al, "Implementation of Both a Second-Moment Closure and a Third-Order Nonlinear Eddy-Viscosity Turbulence Models to KIVA-3V Code", *SAE* 2003-32-0028, JSAE 20034328.

[5] A. A. Amsden, P. J. O'Rourke and T. D. Butler, "KIVA-II: A Computer Program for Chemically Reactive Flows with Sprays", LA-11560-MS, Los Alamos National Laboratoty, May, (1989).

[6] A. A. Amsden, "KIVA-3: A KIVA Program with Block-Structured Mesh for Complex Geometries", LA-12503-MS, Los Alamos National Laboratory, March (1993).

[7] A. A. Amsden, "KIVA-3V: A Block-Structured KIVA Program for Engines with Vertical or Canted Valves", LA-13313-MS, Los Alamos National Laboratory, July, (1997).

[8] N. G. Wright and G. J. Easom, "Non-linear k–e turbulence model results for flow over a building at full-scale", *Applied Mathematical Modeling*, Vol. 27, No. 12, pp. 1013-1033, (2003).

[9] M. Saghafian et. al, "Simulation of Turbulent Flows around a Circular Cylinder Using Nonlinear Eddy-Viscosity Modelling: Steady and Oscillatory ambient Flows", *Journal of Fluid and Structures*, Vol. 17, No. 8, pp. 1213-1236, (2003).

[10] P. Ouellette and P. G. Hill, "Turbulent Transient Gas Injections," *Journal of Fluids Engineering*, Vol. 122, No. 4, p. 743, (2000).